

THE INTERFACE OF REACTIVE- AND MELT PROCESSED POLYAMIDE-6 COMPOSITES

[Kjelt van Rijswijk], Julie J.E. Teuwen, Harald E.N. Bersee and Adriaan Beukers*
K.vanRijswijk@TUDelft.NL

Design and Production of Composite Structures, Faculty of Aerospace Engineering,
Delft University of Technology

* Fellow of the Doshisha University, Kyoto, Japan

Keywords: *Vacuum infusion, thermoplastic composites, anionic polyamide-6, coupling agents.*

Abstract

One of the advantages of reactive processing of thermoplastic composites is that due to *in situ* polymerization of a thermoplastic resin, interfacial bond formation occurs at a higher extend that can be achieved with melt processing. In other words, a thermoplastic composite can be obtained with an interface that is typical for thermoset composites. This paper assesses the effect of the interface on the mechanical performance of a reactively processed and a melt processed polyamide-6 composite. It will be shown that a strong interface especially beneficial for reducing the void content and improving the fatigue performance.

1 General Introduction

In order to manufacture thicker, larger and more integrated thermoplastic composite (TPC) parts, a vacuum infusion process for TPCs is currently being developed at the Delft University of Technology. The research focuses on using an anionic polyamide-6 (APA-6) casting resin (AP Nylon, Brüggemann Chemical, Germany), see Figure 1. At temperatures ranging from 150-190°C, the caprolactam monomer polymerizes into highly crystalline PA-6 in 5-20 minutes using a specifically for this processed developed combination of a carbamoylcaprolactam activator and a magnesium bromide caprolactamate initiator [1]. Because processing takes place below the crystallization temperature of the final polymer, polymerization and crystallization occur simultaneously [2], which means that the fully crystallized composites can be demoulded hot.

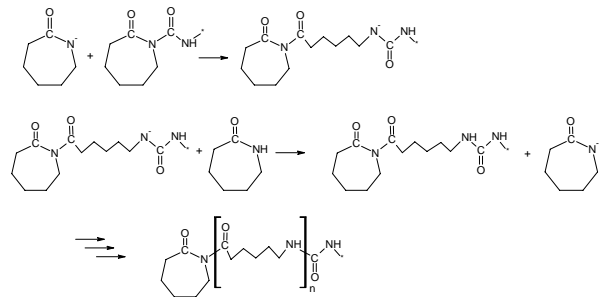


Fig. 1. Anionic polymerization of caprolactam into polyamide-6 using a carbamoylcaprolactam activator.

In this paper, the effect of applying a coupling agent to the glass fibers on the void content and the mechanical properties (static and dynamic) of APA-6 glass fiber composites is discussed. A comparison is made with a traditionally melt-processed PA-6 composite (HPA-6). It will be shown that reactive processing leads to thermoplastic composites with improved mechanical properties.

2 Experimental

2.1 Materials

Together with the caprolactam monomer, a hexamethylene-1,6-dicarbamoylcaprolactam activator was used (HDCL, Brüggolen C20) and a caprolactam magnesium bromide initiator (MgBrCL, Brüggolen C1), all kindly supplied by Brüggemann Chemical, Germany. A resin formulation containing 1.2mol% activator and 1.2mol% initiator relative to the amount of caprolactam was used.

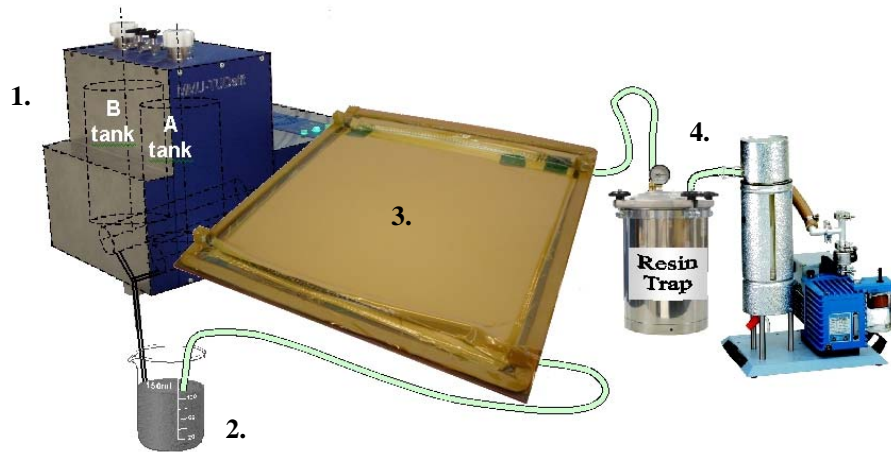


Fig. 3. Processing schematics for infusion of APA-6 composites: (1) mini mixing unit “MMU-TU Delft”, (2) resin buffer, (3) mould and heating system, and (4) pressure control system.

2.2 Processing methods

The composites analyzed in this paper are all balanced and symmetrical laminates consisting of 12 plies of 8-harness satin weave E-glass fabrics (SS 0303 050, weave style 7781, 300 gram/m², Ten Cate Advanced Composites, Nijverdal, The Netherlands). The fabric selected is coated with aminosilanes (see Figure 2), commonly known to be compatible with polyamide-6 (PA-6) matrices. Special care was taken to maintain a constant fiber volume content in order to make a comparison possible.

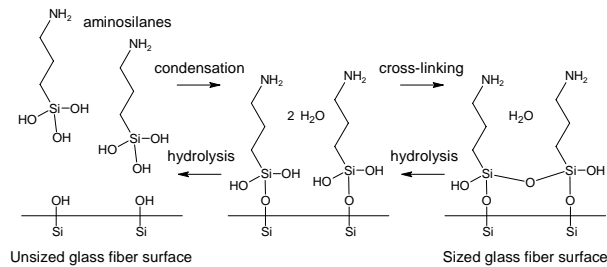


Fig. 2. Sizing of glass fibers with aminosilane coupling agents.

2.2.1 Vacuum infused APA-6 composites (APA-6/GF)

The APA-6 resin material was prepared in the mini mixing unit (MMU), see Figure 3. After dispensing the reactive mixture in the resin buffer (110°C, nitrogen protective atmosphere) degassing took place for 5 minutes at 10 mbar. The vacuum bagged and pre-heated (160-190°C) glass fabrics

were infused at 250 mbar. The composites were allowed to cure for 60 minutes before being demolded to make sure that the composites have reached both their final conversion and crystallinity.

2.2.2 Thermoformed HPA-6 composites (HPA-6/GF)

Hydrolytic polyamide-6 composites (HPA-6/GF) were produced by thermoforming a stack of alternating layers of glass fabrics and dried PA-6 films (Akulon F132-E, DSM, The Netherlands) in a hot flat platen press (LAP 100, Gottfried Joos Maschinenfabrik GmbH & Co, Germany). The laminate was heated up from room temperature to 275°C at a rate of 9°C/min and kept at that temperature for 10 minutes before being cooled down to room temperature at a rate of 20°C/min.

2.3 Analysis methods

2.3.1 Degree of conversion (DOC)

Composite samples were chopped into thin flakes ($t < 0.5$ mm), weighed (m_{tot}) and refluxed overnight in demineralized water. After drying, samples were weighed again. Whereas the monomer caprolactam dissolves easily in water, the polyamide-6 does not and the resulting reduction in mass can be attributed to the monomer (m_{mon}). Additionally, the fiber weight content was determined in a subsequent step by thermal cleaning at 565°C followed by cooling in a dessicator prior to weighing (m_f). The degree of conversion (DOC) was determined according to Eq. 1.

$$DOC = 100 - \frac{m_{mon}}{m_{tot} - m_f} \cdot 100\% \quad (1)$$

2.3.2 Differential Scanning Calorimetry (DSC)

A Perkin Elmer Differential Scanning Calorimeter (DSC-7) was used to measure the degree of crystallinity (X_c) and melting point (T_m) of disc shape specimens ($\varnothing 5$ mm, $m_{disc} \approx 50$ mg) that were punctured out of composite panels and dried overnight at 50°C in a vacuum oven. Samples were first held for 2 minutes at 25°C before being heated to 240°C at $10^\circ\text{C}/\text{min}$. Afterwards, the fiber content (m_f) of the disc shape specimen was determined in a Perkin Elmer Thermal Gravimetric Analyzer (TGA-7). Finally, X_c was calculated and corrected for the degree of conversion (DOC, see Eq.1) according to Eq.2.

$$X_c = \frac{\Delta H_m}{\Delta H_{100}} \cdot \frac{m_{disc}}{m_{disc} - m_f} \cdot \frac{1}{DOC/100} 100\% \quad (2)$$

In which ΔH_{100} is the melting enthalpy of fully crystalline PA-6: $\Delta H_{100} = 190$ J/g [3].

2.3.3 Determination of density, void content and fiber content

First, the density of composite samples ($\rho_{c_measured}$) was determined by displacement according to ASTM D792 (Test Method A) using a Mettler AG204 DeltaRange[®] microbalance. Prior to testing, all specimens were dried in a vacuum oven at 50 mbar and 70°C for at least 85 hours. Second, the fiber weight content (W_f) was determined by thermal cleaning at 565°C followed by cooling in a desiccator prior to weighing. The density of the matrix (ρ_m) was calculated from the densities at 23°C of the monomer ($\rho_{mon} = 1.06$ g/cm³), the amorphous phase of the polymer ($\rho_{am} = 1.08$ g/cm³) and crystalline phase ($\rho_{cr} = 1.24$ g/cm³, α -phase) using the rule of mixtures and the results of previously conducted crystallinity (X_c) and conversion (DOC) measurements, see Eq.3 [4]. After calculating the density of the composite ($\rho_{c_calculated}$) in a similar way according to Eq. 4, the void content (V_v) was determined with Eq.5. The density of the glass fabrics ($\rho_f = 2.62$ g/cm³) was provided by the manufacturer.

$$\rho_m = (1 - DOC) \cdot \rho_{mon} + DOC \cdot X_c \cdot \rho_{cr} + DOC \cdot (1 - X_c) \cdot \rho_{am} \quad (3)$$

$$\rho_{c_calculated} = W_f \cdot \rho_f + (1 - W_f) \cdot \rho_m \quad (4)$$

$$V_v = \frac{\rho_{c_calculated} - \rho_{c_measured}}{\rho_{c_calculated}} \cdot 100\% \quad (5)$$

2.3.4 Short beam shear testing

The short beam shear tests were conducted on a Zwick-Roell Z250 25 ton force machine according to the ASTM D-2344 norm. A three point bending jig equipped with 3mm diameter supports and a 6mm diameter loading nose was adjusted to a span of 11 mm to perform tests on rectangular shape specimens (16 x 5.5 x 2.7 mm). From the maximum force (F_m), the inter laminar shear strength (ILSS) was calculated according to Eq.6.

$$ILSS = \tau_3 = 0.75 \frac{F_m}{w \cdot t} \quad (6)$$

in which w and t are the width and thickness of the test specimen. A minimum of 5 specimens was tested.

2.3.5 Tensile testing

Tensile tests were conducted on a Zwick-Roell Z250 25 ton force machine equipped with extensometers according to ISO 527. Rectangular specimens (Type 3, 250 x 25 x 2.7 mm) with a $0^\circ/90^\circ$ fiber orientation were used with bonded end tabs. A minimum of 5 specimens was tested at a crosshead speed of 2 mm/min. When failure occurred within 10 mm of the grips the test results were discarded.

2.3.6 Compressive testing

Compression tests were conducted on a Zwick-Roell Z250 25 ton force machine equipped with extensometers according to ISO 14126 (Method 2) and ASTM D695. Rectangular specimens (75 x 15 x 2.7 mm) with a $0^\circ/90^\circ$ fiber orientation were used with bonded end tabs. Special care was taken to obtain specimens with parallel end surfaces. A maximum gage length of 10 mm was determined at which Euler buckling was prevented. A minimum of 5 specimens was tested at a

crosshead speed of 1 mm/min. When failure occurred outside the gage length the test results were discarded.

2.3.7 In-plane shear testing

Shear tests were conducted on a Zwick-Roell Z250 25 ton force machine equipped with extensometers according to ISO 14129. Rectangular specimens (250 x 25 x 2.7 mm) with a $\pm 45^\circ$ fiber orientation were used with bonded end tabs. A minimum of 5 specimens was tested at a crosshead speed of 2 mm/min. When failure occurred within the grips the test results were discarded.

2.3.8 Fatigue testing

Tension-tension fatigue testing ($R = 0.1$) was conducted on a MTS 831 Elastomer Test System with 647 Hydraulic Wedge Grips (1 MPa clamping force) according to ASTM D3479/D3479M. A minimum of 5 samples (75 x 10 x 2.9 mm, with end tabs, gage length: 10 mm) was tested per amplitude at 10 Hz (sinusoidal).

2.3.9 Microscopy

A Jeol JSM-840 scanning electron microscope (SEM) was used to analyze the fracture surface of composite specimen. Samples were gold covered by a Balzers Union SCD 040 gold sputter coater prior to analysis.

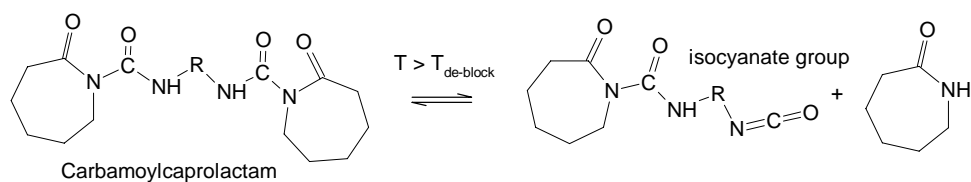
3 The fiber-to-matrix interface of APA-6 composites

In this section, the mechanism of interfacial bond formation in APA-6 composites is presented and the effects (both positive and negative) of interfacial bonding on the processing method and the bulk matrix properties are explained. The overall contribution of the interface on the mechanical properties of the composite are discussed in section 4 by means of a comparative study.

3.1 Interfacial bond formation

The formation of chemical bonds between the aminosilane sizing and the APA-6 matrix is formed in a similar way as branching occurs in the neat resin [2], see Figure 4: de-blocking of the carbamoyl activator at temperatures in excess of its de-blocking temperature generates isocyanate groups, which can form urea linkages with the aminosilanes on the glass surface. The fact that isocyanates already rapidly react with amines at temperatures as low as 60 to 80°C [5], confirms that this reaction with the aminosilanes is likely to occur. Due to the difunctional nature of the activator, initiation of the anionic polymerization of caprolactam is still possible, which causes the polymer chains to grow from the fiber surface ultimately forming an interpenetrating network with the chains in the bulk matrix. As a consequence, the inter laminar shear strength (ILSS) of APA-6 composites increases tremendously when using a coupling agent, see Figure 5.

Step 1: De-blocking



Step 2: Formation of fiber-to-matrix bond

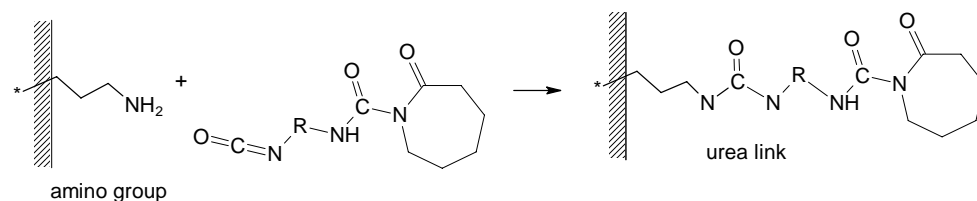


Fig. 4. De-blocking of carbamoylcaprolactam (step 1) and the subsequent formation of fiber-to-matrix bonds (step 2).

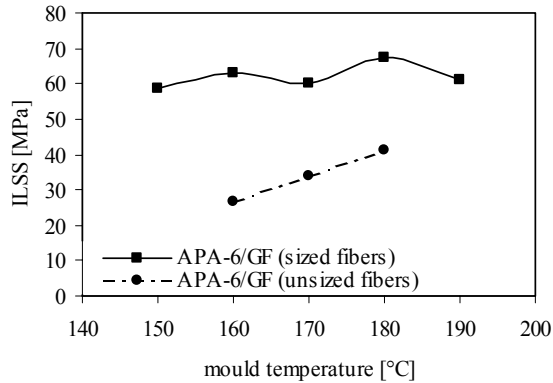


Fig. 5. The effect of the aminosilane coupling agent on the inter laminar shear strength (ILSS) of APA-6 composites.

Although the formation of interfacial bonds is undeniable beneficial for the overall performance of the composites, in the case of APA-6 composites there are a few consequences, which are discussed next.

3.2 The effect of interfacial bonding on the processing method

3.2.1 Reduction of the infusion window

According to the chemical bonding mechanism in Figure 4, the fiber-to-matrix interface should improve at a higher processing temperature:

- Because the equilibrium (step 1, Figure 4) shifts to the right with increasing temperature, de-blocking of the activator occurs to a larger extend, which increases the chance of bond formation with the fibers.
- At higher temperatures the chains initiated at the fiber surface can reach longer lengths and interpenetrate with the bulk matrix at a higher level before crystallization ‘freezes’ the matrix.

At a higher processing temperature, however, APA-6 polymerizes faster, which reduces the available time for infusion.

3.2.2 Activator depletion

As shown in Figure 4, with every interfacial bond that is formed, the total number of activator groups is reduced by one. In order to prevent

activator depletion, extra activator has to be added to the APA-6 resin prior to infusion. Whereas for the manufacturing of neat APA-6 products 0.6mol% activator is sufficient [2], manufacturing of composites requires double this amount. Table 1 shows that unsized fibers lead to low conversions, which is caused by the fact that without interfacial bond formation an activator overdose remains. As was explained in a previous publication [2], a too high activator concentration results in extensive oligomer formation (low molecular weight fractions), which causes the conversion to drop. This clearly shows that fine-tuning of the formulation in accordance with the fiber content in order to obtain the optimum activator concentration after infusion is essential for obtaining a high degree of conversion.

Table 1. The effect of the aminosilane coupling agent on the conversion and crystallinity of APA-6 composites.

T_{mould} [°C]	Conversion [wt%]		Crystallinity [wt%]	
	sized	unsized	sized	unsized
160	96	91	41	44
170	95	90	38	43
180	93	93	32	38

3.3 The effect of interfacial bonding on the bulk matrix properties

3.3.1 Reduction of the degree of crystallinity

As mentioned in section 3.1, interfacial bond formation follows the same mechanism as the formation of branch-points in neat APA-6. In other words, an APA-6 composite with a strong chemical interface has a highly branched bulk matrix. As was demonstrated by Risch et al., the majority of the bulky branch-points is not incorporated into the lamellar crystals and consequently decreases the degree of crystallinity [5]. A second reason for a lower degree of crystallinity is the reduced mobility of chains that are attached to the fibers. Table 1 shows for the same processing conditions, sized fibers lead to a lower degree of crystallinity than unsized fibers. As for all semi-crystalline polymers, a reduction in crystallinity is accompanied by a lower modulus and a reduction in chemical resistance, of which the consequences are explained in section 4.

3.3.2 Reduction of the void content

Because the crystalline phase has a higher density than the amorphous phase (1.24 vs. 1.08 g/cm³ [6]), crystallization-induced resin shrinkage is inevitable, which is a common source for voids in composites. As mentioned in the previous paragraph, the formation of interfacial bonds (and the simultaneous occurrence of branching) reduces the degree of crystallinity and hence the void content.

4 Composite properties

It will be demonstrated in this section that reactive processing leads to a PA-6 composite with a stronger fiber-to-matrix interface than can be achieved during melt-processing. The drawback of such a strong interface, however, is that it reduces the degree of crystallinity and consequently the modulus of the matrix, as explained in the previous section. A compromise between maximizing the matrix properties and maximizing the interfacial strength is inevitable in order to maximize the properties of the entire composite: a relatively low mould temperature results in a high degree of crystallinity and a weak interface, whereas a high mould temperature results in a low crystallinity and a strong interface. This section compares the properties of a melt processed HPA-6 composite and an APA-6 composite infused at 170°C, which is an intermediate mould temperature.

Table 2. Physical properties of an infused APA-6 composite and a thermoformed HPA-6 composite.

Physical property	APA-6/GF	HPA-6/GF
Thickness [mm]	2.8	2.7
Density [g/cm ³]	1.8	1.9
Fiber content [v%]	50	51
Void content [%]	3.0	1.3
Conversion [%]	95	100
Crystallinity [%]	35	33
Melting point [°C]	217	220

4.1 Physical composite properties

The physical properties of both composites are summarized in Table 2. It can be seen that tailoring the processing parameters indeed resulted in more or less equal fiber volume content. The

relatively high void content and crystallinity of the APA-6 composites form an indication of a weak fiber-to-matrix bond, as explained in section 3. The lower melting point of the APA-6 composites compared to its melt processed counterpart is a direct result of the occurrence of branching in the bulk matrix and the presence of 5 wt% residual monomer.

4.2 Mechanical properties: dry as molded values

For dry as molded conditions, the static mechanical properties of the composites are presented in Table 3, whereas the S-n curves, or Wöhler curves, for tension-tension fatigue are shown in Figure 6.

4.2.2 Static properties

Table 3 shows that the tensile strength of the composites, which is a typical fiber dominated property, differs for both matrices. Because the tensile strength decreases with the viscosity of the matrix during processing ($\eta_{\text{APA-6}} = 0.01 \text{ Pa}\cdot\text{s}$, $\eta_{\text{HPA-6}} = 200 \text{ Pa}\cdot\text{s}$) it is assumed that the decrease in tensile strength is related to fiber waviness: the higher the viscosity of the matrix, the more the fibers are pushed aside during impregnation and the higher the degree of misalignment of the fibers in the final composites, which is obviously detrimental for the tensile properties. Misalignment of fibers should have the same effect on the compressive properties and indeed a similar viscosity-related trend is found in the compressive strength. The remark is made that in general the influence of the matrix modulus on the compressive strength is much larger than on the tensile strength. In this case, the higher the matrix modulus (higher crystallinity, see Table 2), the higher indeed the compressive strength of the composite.

Table 3. Static mechanical properties of an infused APA-6 composite and a thermoformed HPA-6 composite (dry as molded properties).

Mechanical Property	APA-6/GF	HPA-6/GF
Compressive strength [MPa]	473	390
Compressive modulus [GPa]	26	25
Tensile strength [MPa]	495	456
Tensile modulus [GPa]	26	26
In-plane shear strength [MPa]	127	117
In-plane shear modulus [GPa]	4.1	3.7
ILSS [MPa]	69	65

4.2.2 Dynamic properties

From the previous section, it can be concluded that in dry as molded conditions, a high degree of crystallinity is of paramount importance for the static mechanical performance of thermoplastic composites as it results in a high matrix modulus.

Dynamic testing, however, shows a different ranking as is shown in Figure 6. The HPA-6 composite has a marginally better resistance against fatigue, which is expected to be caused by the fact that APA-6/GF ($T_{mould} = 170^{\circ}C$) has substantially more initial defects (voids, unreacted monomer), which is beneficial for crack initiation and leads to a reduction in fatigue life [8]. Subsequent crack surface analysis revealed bare fibers and extensive fiber pull-out for both composites, see Figure 7, which indicates a poor fiber-to-matrix interface. Apparently cracks grow along this interface until failure occurs.

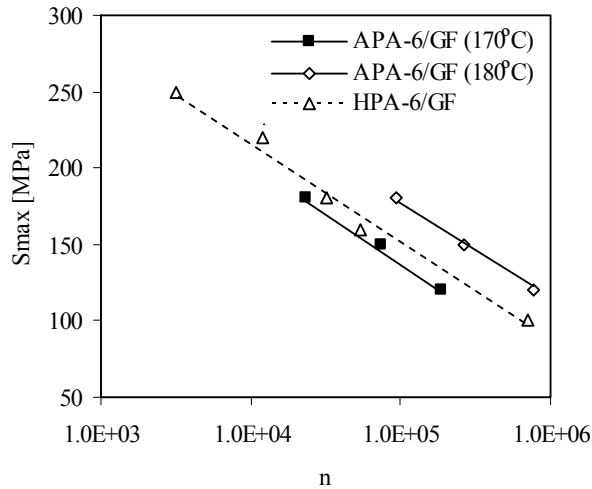


Fig. 6. S-n curves of three PA-6 composites tested in this research.

To assess the importance of the fiber-to-matrix interface on the fatigue resistance, an additional APA-6 composite ($T_{mould} = 180^{\circ}C$) was included in the dynamic test program. Due to the higher mould temperature, this composite has a stronger fiber-to-matrix interface. The increase in performance (see Figure 6) shows the importance of the formation of interfacial bonds on the fatigue performance of composites. This is

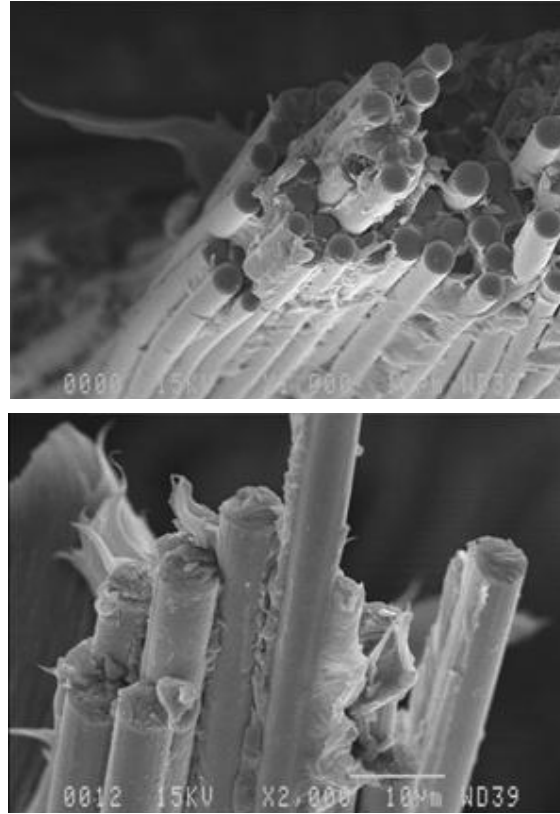


Fig. 7. SEM micrographs of the fracture surface of APA-6/GF cured at 170°C (top) and HPA-6/GF (bottom) after fatigue testing.

especially true for APA-6 composites as chemical bond formation also reduces the void content. Chemical bond formation also has an effect on the failure mode as is shown in Figure 8: after failure, the fibers are still covered by matrix, which indicates that instead of following the interface, the cracks are forced to progress through the ductile matrix. The appearance of striations confirms this as these form the classic fingerprint of ductile materials when failed under cyclic loading [9].

4.3 Mechanical properties: moisture conditioning

Whereas the amorphous phase of APA-6 is capable of absorbing a vast amount of water, the crystalline phase cannot and, therefore, a higher the degree of crystallinity reduces the total amount of moisture that is absorbed by the matrix. Because water acts as a plasticizer for PA-6, a high degree of crystallinity is beneficial for retaining strength and stiffness in humid conditions [7].

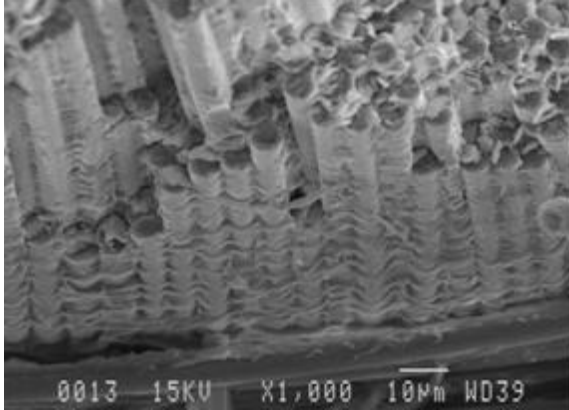


Fig. 8. SEM micrograph of the fatigue fracture surface of APA-6/GF manufactured at 180°C.

Figure 9 shows that when tested in dry conditions reactively processed APA-6 composites have a higher ILSS than their melt processed HPA-6 counterpart due to their strong interface. Because the formation of interfacial bonds significantly reduces the crystallinity of the APA-6 matrix, the matrix becomes more susceptible to moisture absorption, which causes a steep drop in ILSS. Also the lower void content of the melt-processed PA-6 composites contributes positively to retention of properties when moisture conditioned.

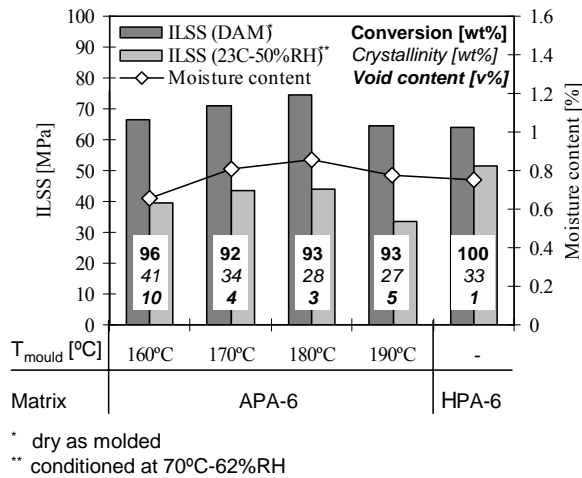


Fig.9. The effect of moisture conditioning on the interlaminar shear stress (ILSS) of reactively processed APA-6 composites and melt processed HPA-6 composites.

5 Conclusions

Reactive processing improves the properties of APA-6 composites as it results in strong chemical bonds between the fibers and the matrix at a level that cannot be achieved with traditional melt-processing. As a consequence, the APA-6 composites outperform their melt-processed HPA-6 counterpart in all static and dynamic mechanical tests conducted. The large number of interfacial bonds, however, reduces the degree of crystallinity, which makes APA-6 composites more susceptible to moisture absorption.

References

- [1] K. van Rijswijk, H.E.N. Bersee, W.F. Jager and S.J. Picken. "Optimisation of Anionic Polyamide-6 for Vacuum Infusion of Thermoplastic Composites: Choice of Activator and Initiator". *Composites Part A*, 37, 949-956, 2006.
- [2] K. van Rijswijk, H.E.N. Bersee, A. Beukers, S.J. Picken and A.A. van Geenen. "Optimisation of Anionic Polyamide-6 for Vacuum Infusion of Thermoplastic Composites: Influence of Polymerisation Temperature on Matrix Properties". *Polymer Testing* 25:392-404, 2006.
- [3] Cartledge, H., C.A. Baillie. "Studies of Microstructural and Mechanical Properties of Nylon/Glass Composites. Part I: The Effect of Thermal Processing on Crystallinity, Transcrystallinity and Crystal Phases". *Journal of Materials Science* 34(20):5099-5111, 1999.
- [4] Vlasveld, D.P.N., J. Groenewold, H.E.N. Bersee, E. Mendes, S.J. Picken. "Analysis of the Modulus of Polyamide-6 Silicate Nanocomposites using Moisture Controlled Variation of the Matrix Properties". *Polymer* 46:6102-6113, 2006.
- [5] Randall, D., S. Lee. "The Polyurethanes Book". NY, John Wiley & Sons, Ltd, 2002.
- [6] Risch, B.G., G.L. Wilkes, J.M. Warakomski. "Crystallization Kinetics and Morphological Features of Star-Branched Nylon-6: Effect of Branch-Point Functionality". *Polymer* 34(11):2330-2343, 1993.
- [7] K. van Rijswijk, S. Lindstedt, D.P.N. Vlasveld, H.E.N. Bersee and A. Beukers. "Reactive Processing of Anionic Polyamide-6 for Application in Fibre Composites: a Comparative Study with Melt Processed Polyamides and Nanocomposites". *Polymer Testing* 25: 873-887, 2006.
- [8] Talreja, R. "Fatigue of Composite Materials: Analysis, Testing and Design". Lancaster, Technomic, 1990.
- [9] Carlson, R.L., G.A. Kardomateas. "Introduction to Fatigue in Metals and Composites". London, Chapman and Hall, 1996.